THE JOURNAL OF PHYSICAL CHEMISTRY B

Article

pubs.acs.org/JPCB

Tetracycline-Loaded Biomimetic Apatite: An Adsorption Study

Sophie Cazalbou,[†] Ghislaine Bertrand,[‡] and Christophe Drouet*[,‡]

[†]CIRIMAT Carnot Institute, UMR CNRS/INPT/UPS 5085, Faculté des Sciences Pharmaceutiques, University of Toulouse, 35 Chemin des Maraîchers, 31400 Toulouse, France

[‡]CIRIMAT Carnot Institute, UMR CNRS/INPT/UPS 5085, University of Toulouse, Ensiacet, 4 allée E. Monso, 31030 Toulouse cedex 4, France

ABSTRACT: Biomimetic apatites are appealing compounds for the elaboration of bioactive bone-repair scaffolds due to their intrinsic similarity to bone mineral. Bone surgeries are however often heavy procedures, and the infiltration of pathogens may not be totally avoided. To prevent their development, systemic antibiotic prophylaxis is widespread but does not specifically target surgical sites and involves doses not always optimized. A relevant alternative is a preliminary functionalization by an infection-fighting agent. In this work, we investigated from a physicochemical viewpoint the association of a wide-spectrum antibiotic, tetracycline (TC), and a biomimetic nanocrystalline apatite previously characterized. TC adsorption kinetics and isotherm were thoroughly explored. Kinetic data were fitted to various models (pseudo-first-order, pseudo-second-order, general kinetic model of order *n*, Elovich, double-exponential, and purely diffusive models). The best fit was found for a double-exponential kinetic model or with a decimal reaction order of 1.4, highlighting a complex process with such TC molecules which do not expose high-affinity end groups for the surface of apatite. The adsorption isotherm was perfectly fitted to the Sips (Langmuir−Freundlich) model, while other models failed to describe it, and the Sips exponent greater than unity (1.08) suggested a joint impact of surface heterogeneity and positive cooperativity between adsorbed molecules. Finally, preliminary insights on TC release from pelletized nanocrystalline apatite, in aqueous medium and neutral pH, were obtained using a recirculation cell, indicating a release profile mainly following a Higuchi-like diffusion-limited rate. This work is intended to shed more light on the interaction between polar molecules not exhibiting high-affinity end groups and biomimetic apatites and is a starting point in view of the elaboration of biomimetic apatite-based bone scaffolds functionalized with polar organic drugs for a local delivery.

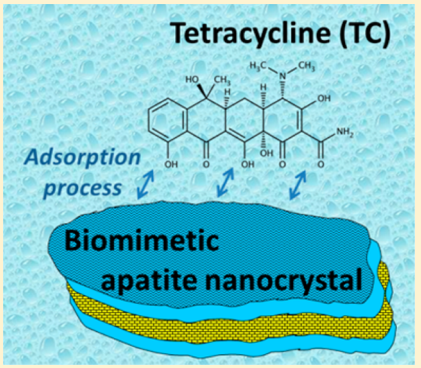

1. INTRODUCTION

Calcium phosphate apatites, deriving from hydroxyapatite (HA), $Ca_{10}(PO_4)_6(OH)_2$, are appealing candidates for the preparation of bone-related scaffolds due to their intrinsic similarity with the mineral part of bones.[1,2] So-called "biomimetic" synthetic apatites analogous to bone mineral may be produced based on (i) good knowledge of the physicochemical characteristics of biological apatites and (ii) an appropriate control on synthesis (and eventual post-treatments) conditions, as shown previously.[2,3] As for bone apatites, these biomimetic analogs are nanocrystalline and nonstoichiometric and exhibit a high surface reactivity directly linked to the presence, on the nanocrystals, of a nonapatitic hydrated layer containing labile ions.[4,5] This surface reactivity has been shown to allow the preparation of apatite nanocrystals functionalized with various types of ions or (bio)molecules of interest: for instance, the association of antibacterial enzymes,[6] bisphosphonate,[7,8] growth factor,[9,10] bioactive ions (e.g., Sr^{2+}, Mg^{2+}),[11] or anticancer drugs[12,13] has been reported. Such associations are facilitated by the existence of charged (end) groups and especially of anionic chemical functions (such as phosphate, phosphonate, or else carboxylate) from the adsorbate and surface ions located on apatite (nano)crystals.[14] This is especially the case for the above references. Further insights on surface aspects and surface functionalization of apatitic systems can be found in more depth elsewhere.[14,15]

The possibility to confer additional functionalities such as antimicrobial properties, improved osteoconduction/osteoinduction, etc., to biomimetic apatite-based systems can therefore be seen as a resourceful way to tailor bone-repair biomaterials in regard to the patients' needs. In particular, adjoining antibacterial properties to biomimetic apatite scaffolds appears especially appealing in view of combining the good osteointegration/conduction/induction features of nanocrystalline apatites[9] with the antibacterial properties of an associated agent. This is all the more relevant since bone surgery often implies heavy procedures where the risk of infiltrating pathogens (e.g., *Staphylococcus aureus, Staphylococcus epidermidis*...) may not a priori be totally eliminated. Also, installed bone infections appear difficult to eradicate due to bone porosity, thus suggesting that infection *prevention* should be privileged. Although the use of systemic administration of antibiotics is broadly performed, it cannot target the surgical area and the determination of adapted doses remains delicate. The

Received: November 21, 2014
Revised: January 19, 2015

DOI: 10.1021/jp5116756
J. Phys. Chem. B XXXX, XXX, XXX−XXX

possibility to convey directly to the implanted biomaterial some antimicrobial functions is thus particularly attractive. One way to achieve this goal is to associate (limited amounts of) antibiotics in a controlled manner. The concept of associating antibacterial drugs to bone-related biomaterials is not new per se (see for example refs 16−18), but the use of biomimetic nanocrystalline apatites that mimic the characteristics of bone apatite has not been widely addressed as yet and still deserves attention. This is the topic of the present physicochemical study, where the adsorptive behavior (in terms of kinetics of adsorption, adsorption isotherm, and preliminary desorption aspects) of one of the most widely used wide spectrum antibiotic drugs, tetracycline or TC (active against various Gram-negative and Gram-positive microorganisms, already used in some scaffold formulations[19,20]), onto a biomimetic nanocrystalline apatite was investigated in depth. Besides the use of a biomimetic apatite substrate for associating an antibiotic agent such as tetracycline, one additional particularity of this work is to analyze the adsorptive behavior of a molecule that does not expose any "high-affinity" charged end group (such as phosphates, phosphonates, carboxylates; see, for example, ref 14) and for which the adsorption process is bound to be guided only by the presence of polar functional groups, which has rarely been addressed to our knowledge in the literature.

2. MATERIALS AND METHODS

2.1. Synthesis of the Nanocrystalline Apatite Substrate. The "model" nanocrystalline apatite sample used as adsorption substrate in this study was obtained by precipitation at room temperature and close to physiological pH (7.2), the latter being ensured by an excess of phosphate ions in the medium. Two starting solutions were used: solution A contained calcium nitrate tetrahydrate (Merck Emsure grade, purity 99.0%) as calcium source (calcium concentration of 0.3 M), and solution B contained diammonium hydrogen phosphate (VWR Normapur grade, purity 99.0%) as phosphate source (phosphate concentration 0.6 M). After rapidly pouring solution A into solution B and mixing, the precipitate was left to mature for 1 day prior to filtration on a Büchner funnel, washing with deionized water, and freeze drying, leading to a powder sample used as such in the adsorption study.

2.2. Physicochemical Characterization. The physicochemical characteristics of the apatite substrate were drawn from complementary analyses. Structural features were investigated by way of X-ray diffraction (XRD) on an INEL 120 CPS diffractometer (cobalt radiation, λ_{Co} = 1.78892 Å). Fourier transform infrared (FTIR) spectra were recorded on a Nicolet 5700 spectrometer in the range 400−4000 cm^{-1} (64 scans, at a resolution of 4 cm^{-1}). Calcium and orthophosphate ($PO_4^{3-}$and HPO_4^{2-}) ionic contents were determined after dissolution of the apatite powder in perchloric acid, respectively, by EDTA complexometry and visible spectrophotometry (using the phospho−vanado−molybdenic complex, at λ = 460 nm).[21] The relative uncertainty on calcium and phosphorus concentrations is evaluated to 0.5%. The specific surface area, S_w, of the sample was determined using the BET method (nitrogen adsorption) on a Nova 1000 Quantachrome apparatus.

Tetracycline (TC) in solution was titrated in this work by UV spectrophotometry (molar absorption coefficient of tetracycline ε = 136 $L{\cdot}mol^{-1}{\cdot}cm^{-1}$), by monitoring the optical density at 355 nm (absorption maximum), and in relation with a calibration curve established between 0 and 1000 mg/L of TC (correlation coefficient 0.9999).

2.3. Tetracycline (TC) Adsorption and Release Experiments. The commercial tetracycline (see Figure 1) used in this

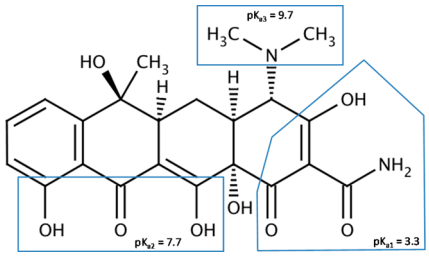

Figure 1. Chemical formula of tetracycline (TC).

work was in the form of the rather soluble tetracycline phosphate salt (Sigma, CAS No. 1336-20-5): 100 mg of compound containing 82 mg of TC. In the text, all TC masses will refer to pure TC and be given in milligrams of tetracycline per liter (= ppm).

Note that "phosphate salt" simply implies that the counterion is of phosphate nature: after immersion, the phosphate counterion dissolves in the medium without being "attached" to the tetracycline molecule, which exhibits the form indicated in Figure 1.

The adsorption study was performed in deionized water at a pH close to neutral and at room temperature (∼22 °C), corresponding to conceivable conditions usable in practice (e.g., by industrial companies) for the preparation of drug-loaded systems. TC adsorption on biomimetic apatite was carried out here in two steps, as indicated below.

First, a kinetic survey was carried out so as to determine the amount of time needed to reach the thermodynamic adsorption equilibrium. To this goal, seven time points were examined, between 15 and 105 min, using in each case 20 mg of apatite suspended in 5 mL of TC solution at a concentration of 820 mg/L (corresponding to 1000 mg/L of the commercial TC phosphate complex). After the selected duration, the sample was immediately isolated from the supernatant by centrifugation (2 min at 5000 rpm), and the supernatant was titrated by UV spectrophotometry as indicated above.

Second, the adsorption isotherm of TC on the biomimetic apatite substrate was established with the same solid/liquid ratio and temperature (22 °C) as for the kinetic study but varying the initial TC concentration in the 0−820 mg/L range (for a contact time of 100 min). As above, each sample was centrifuged and the TC concentration in the supernatant was titrated by UV spectrophotometry.

In each case, the amount of tetracycline (TC) adsorbed on the apatite substrate was determined by difference between the initial TC concentration and the final concentration in the supernatant.

TC release was carried out in deionized water set to pH 7.4 by adequate NaOH or HCl dropwise addition, at room temperature, over a period of 95 h. To this aim, an apatite pellet (13 mm diameter, ∼1 mm thick) was prepared by uniaxial pressing (10 s under 8 tons) of 96 mg of apatite powder preliminarily loaded with adsorbed TC, and the pellet was introduced in a Sotax CE 1 DISSOTEST recirculation cell consisting in a reactor chamber containing the pellet, a reservoir for the medium, an integrated pump, and the necessary tubing (total volume cell + tubing = 50 mL). The TC-loaded apatite

DOI: 10.1021/jp5116756
J. Phys. Chem. B XXXX, XXX, XXX−XXX

sample used in this release experiment was prepared by contacting 200 mg of apatite powder with 50 mL of TC solution (thus keeping the same solid/solution ratio as for the adsorption study) with an initial concentration of 490 mg TC/L. After a contact time of 100 min, the apatite was retrieved by filtration on a Büchner funnel, washing with deionized water, and freeze drying for 22 h (freeze drier set to −80 °C and a residual pressure of 0.1 mbar). A total of 50 mL of recirculating medium (water set to pH 7.4) was used in the recirculation cell at a flow rate of 15 mL/min. At selected time points, 5 mL of medium was sampled and analyzed by UV spectrophotometry as above, for TC titration, and they were replaced immediately by 5 mL of deionized water for maintaining a constant volume throughout each experiment, in accordance with sink pharmaceutical conditions.

3. RESULTS AND DISCUSSION

3.1. Physicochemical Characterization of Apatite Substrate. The apatite sample prepared in this work (apatite matured for 1 day at room temperature) was characterized on a physicochemical basis by way of complementary techniques. XRD analyses pointed to the typical characteristic X-ray diffraction pattern of a low-crystallinity apatitic phase, as in the case of bone apatite. Figure 2 reports the obtained

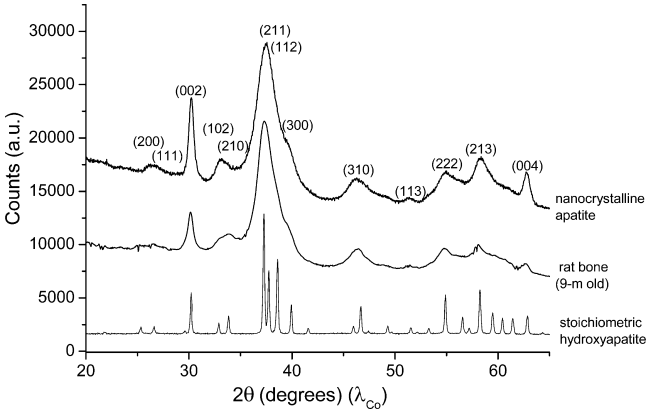

Figure 2. XRD pattern of prepared apatite substrate, in comparison to stoichiometric hydroxyapatite and to rat bone (9 month old).

diffractogram along with that of a "reference" rat bone (femur from male Wistar rat 9 month old). As may be seen, the two XRD patterns show great similarities. In both cases, only apatite peaks could be detected, which may be indexed according to the crystallographic features of hydroxyapatite (hexagonal, space group $P6_3/m$, JCPDS file 09-432). The observed low degree of crystallinity in such apatite compounds—whether of biological origin or for synthetic biomimetic analogs—was shown to be assignable to both the nanometer-scale dimensions of constitutive crystals and some intrinsic crystal disorder, as discussed in detail elsewhere.[3] Application of Scherrer's formula to diffraction lines (002) and (310) led to an approximation of the mean crystallite dimensions on the order of 20 and 5 nm (±0.5 nm), respectively, in terms of mean lengths and widths, which confirms the nanocrystalline character of the precipitated apatite compound.

FTIR spectra were then recorded for this apatite sample. The vibrational signature of calcium phosphate apatite was confirmed, and the main absorption bands have been indexed in Figure 3 (see ref 22 for detailed vibrational band

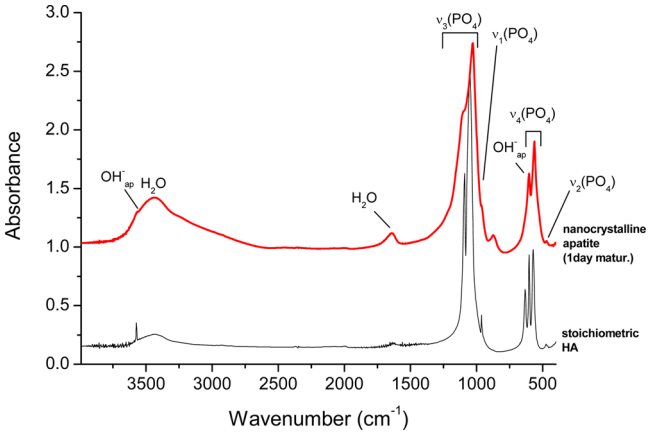

Figure 3. FTIR spectrum for precipitated nanocrystalline apatite and comparison with stoichiometric hydroxyapatite (HA).

attributions). Note that in this figure, contrary to what was done for XRD, the case of rat bone has not been plotted as it displays various bands attributable to collagen which then superimpose with the bands of the apatitic phase. The presence of absorptions around 535 and 875 cm^{-1}, characteristic of HPO_4^{2-} ions (in such noncarbonated apatites), as well as the low intensity of OH^- vibration bands (especially the OH libration[23] band at 632 cm^{-1}) point out the nonstoichiometric character of this apatite compound, as for bone apatite.[24,25]

In order to inspect further the nonstoichiometry of this apatite compound, chemical analyses were carried out to determine its overall Ca/P molar ratio. The experimental value reached, i.e., Ca/P ≅ 1.46 ± 0.02, was found to be significantly lower than the one (1.67) characteristic of stoichiometric hydroxyapatite, thus confirming the presence of ion vacancies, especially in calcium sites. Such low Ca/P ratios are also observed in bone apatite.[15,25]

All these XRD, FTIR, and chemical analysis results thus highlight the "biomimetic-like" character of this apatite sample, thanks to evident similarities with bone apatite, which may thus be seen as a good candidate for the preparation of bone-repair scaffolds. It thus appears appropriate in the present study that focuses on the adsorption behavior of the antimicrobial drug tetracycline.

3.2. Investigation of TC Adsorption and Release Aspects. *3.2.1. Kinetics of TC Adsorption.* In a first step, the kinetics of adsorption of TC, at room temperature, onto the above-characterized biomimetic apatite substrate was followed (described in the Materials and Methods). Figure 4 reports the observed data plotted in terms of the amount adsorbed vs the contact time in solution. TC adsorption reached quasi-equilibrium in 30 min, which is, for example, faster than TC sorption on clays/montmorillonite.[26,27] Also, the adsorption capacity was around 35 mg/g (see Figure 4), corresponding to value 0.29 mg/m^2, which is, for instance, in the same range as for carbon nanotubes (0.3 mg/m^2), greater than for goethite (0.14 mg/m^2), but lower than for Illite (0.59 mg/m^2).[26−30]

In order to further investigate the kinetics of adsorption between TC molecules and the surface of our biomimetic apatite, the data points were tentatively fitted with various kinetic models. In a first step, the pseudo-first-order and pseudo-second-order kinetic models were considered. Note that, in this context of adsorption kinetics, the prefix pseudo relates to the fact that the considered concentrations are *not for dissolved solutes* in a liquid phase but for *adsorbed* species linked

DOI: 10.1021/jp5116756
J. Phys. Chem. B XXXX, XXX, XXX−XXX

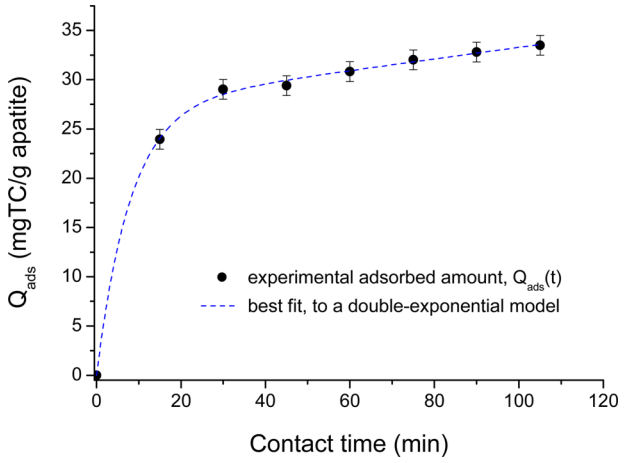

Figure 4. TC adsorption kinetics on 1 day matured biomimetic apatite.

to a solid surface, as was, for example, reminded by Qiu et al.[31] These models were indeed often discussed in the literature by authors trying to fit their kinetic data with relatively simple models. Reviews of various studies where a satisfying fit was found either with the first-order or with the second-order model have been written, whether in the case of the (ad)sorption of ions or of (bio)molecules (see, for example, refs 31−33). These review papers also remind the underlying theoretical background. Briefly, these two models, respectively, correspond to a value of n of 1 and 2 in the following general equation depicting the evolution of the coverage $\theta(t)$ with time

$$\frac{d\theta(t)}{dt} = k_n(1 - \theta(t))^n \quad (1)$$

where n is the adsorption reaction order, $\theta(t)$ is the coverage of the surface at time t (proportion of adsorption sites occupied by adsorbed species), and k_n is the rate constant. This equation can alternatively be rewritten as

$$-\frac{d\lambda(t)}{dt} = k_n \cdot \lambda(t)^n \quad (2)$$

where $\lambda(t)$ is the concentration of available adsorptions sites on the adsorbent surface corresponding to

$$\lambda(t) = 1 - \frac{Q(t)}{Q_{ads,e}} \quad (3)$$

where $Q(t)$ and $Q_{ads,e}$ are, respectively, the adsorbed amounts (generally given in mg/g of adsorbent or in mg/m^2) at time t and at equilibrium. When $n = 1$ (pseudo-first order), integration of eq 2 leads to

$$Q(t) = Q_{ads,e} \cdot [1 - \exp(-k_1 \cdot t)] \quad \text{(pseudo-first order)} \quad (4)$$

while for $n = 2$ (second-order model) we have

$$Q(t) = Q_{ads,e} \cdot \left[1 - \left(\frac{1}{1 + k_2 \cdot t}\right)\right] \quad \text{(pseudo-second order)} \quad (5)$$

These two equations may then allow one to attempt fitting the experimental curve $Q(t) = f(t)$ and conclude on the relevance of these two simple models for defining the adsorption kinetics observed. Interestingly, a literature overview (see, for example, refs 32 and 33) points out the fact that the kinetic model giving the best fit for experimental data points is deeply dependent on the dual adsorbate/adsorbent system: indeed, for a given ion or molecule, a good correlation was reported with either the first-order or the second-order model depending on the nature of the substrate. Thus, it does not appear possible/legitimate to expect that a given ion or molecule will invariably adsorb following one single model: the nature of its interactions with the substrate adsorption sites needs to be taken into account, and it dictates the thermodynamics and kinetics of the adsorption/desorption processes. It is, for example, obvious by comparing the sorption of arsenic(V), cadmium, or chromium(VI), among other metal cations, for various substrates, and which were shown to lead to either first-order (refs 34−36) or second-order (refs 37−39) correlations. The adsorption of tetracycline on various substrates was especially studied in some literature works, and the kinetics were matching with either a first-order model[28] or a second-order one (e.g., refs 27 and 40−42), although the latter seems to be more commonly acknowledged. Similarly, a given type of substrate may lead to different kinds of interactions (and thus kinetic models) depending on the nature of the adsorbing species, which therefore does not allow one to strictly expect experimental data points to follow an unalterable kinetic model. Examples relating to adsorptive processes on apatite compounds which followed either first-order (e.g., ref 43) or second-order (e.g., refs 44 and 45) kinetic models, depending on the nature of the adsorbing species, were, for example, reported.

In the present study, a possible correlation with these two models was checked. The fit parameters which best described the data were determined (using the Origin 8.5 software and its statistical solver) upon minimizing the deviations of the theoretical curve from the experimental points. The goodness of fit was systematically recorded by statistical analysis. Table 1 reports, in particular, the residual sum of squares (RSS) and the adjusted R^2, both values being directly linked to the pertinence of the fit (the former being expected to decrease as close as possible to zero, and the latter to increase up to unity when improving the fit). For a reminder on these statistical outcomes,

Table 1. Statistical Analysis of the Goodness of Fit for TC Adsorption Kinetics on Nanocrystalline Apatite, According to Various Mathematical Models

statistics	first order	second order	general model (order n)[a]	DEM	Elovich	$\sqrt{t}$ variation
no. of points	8	8	8	8	8	8
degrees of freedom (dof-error)	6	6	5	3	6	7
residual sum of squares (RSS)	8.454	2.029	1.536	0.646	2.047	339.266
adjusted R^2	0.9886	0.9973	0.9975	0.9983	0.9972	0.6062

[a] $n = 1.4$ here, see text.

DOI: 10.1021/jp5116756
J. Phys. Chem. B XXXX, XXX, XXX−XXX

readers are invited to consult statistics reference textbooks or publications (e.g., ref 46).

As may be seen in Table 1 by comparing the statistical outcomes of the first- and second-order models, the former cannot describe adequately our experimental data points, suggesting that the reaction order for the adsorption of TC on our biomimetic apatite is different from unity. This is especially evidenced by the significantly large value for the residual sum of squares (RSS). A noticeably increased goodness of fit was on the contrary obtained when fitting our experimental data points with the second-order model, thus suggesting a reaction order greater than 1. In their review paper, however, Liu and Liu[33] point out that "*there is not any theoretical basis for [sorption]* reaction to *be restricted to first- or second-order*". This is an important point that we also believe deserves attention when dealing with kinetic modeling: since the adsorption processes occur on real and often complex systems, often involving heterogeneous solid surfaces and sometimes complex molecules, the idea to limit the fit to only order-1 and order-2 reactions does not seem to be supported by any physical background, and any n value (including decimal ones) could a priori be also acceptable for such complex adsorbate/adsorbent systems. Examples of $n = 1.4$ or 2.1 (n being sometimes called x in publications) were, for example, given for describing ionic sorption.[33] It is then suggested to check also, in every system of interest, the general equation (involving a nonpredetermined value of n), i.e., eq 2, and to determine the most statistically favorable value of n upon mathematical fitting. The idea of checking fits only with the values $n = 1$ and 2 does not appear legitimate: a better comprehension of actual mechanisms may be more easily reached by allowing a nonpredetermined order of reaction.

Solving eq 2 may not appear evident at first glance as it involves simultaneously a continuously varying function, namely, $Q(t)$, and its involving rate of change versus time in the form of its first derivative. It can however be solved by considering it as a differential equation where the "variables" $Q(t)$ and t can be separated. Indeed, the equation

$$-\frac{\mathrm{d}\left(1-\frac{Q(t)}{Q_{\mathrm{ads,e}}}\right)}{\mathrm{d}t} = k_n\cdot\left(1-\frac{Q(t)}{Q_{\mathrm{ads,e}}}\right)^n \tag{6}$$

can be rewritten as

$$-\frac{\mathrm{d}\left(1-\frac{Q(t)}{Q_{\mathrm{ads,e}}}\right)}{\left(1-\frac{Q(t)}{Q_{\mathrm{ads,e}}}\right)^n} = k_n\cdot\mathrm{d}t \tag{7}$$

which can then lead, after integration, to the solutions

$$\frac{\left(1-\frac{Q(t)}{Q_{\mathrm{ads,e}}}\right)^{-(n-1)}}{n-1} = k_n\cdot t + c_n \text{ if } n \neq 1 \tag{8}$$

and

$$-\ln\left(1-\frac{Q(t)}{Q_{\mathrm{ads,e}}}\right) = k_n\cdot t + c_n \text{ if } n = 1 \tag{9}$$

In the latter case (eq 9, where $n = 1$), we find again eq 4 (by taking the exponential of both terms and rearranging the equation and keeping in mind that at time zero, $Q(0) = 0$, leading in this case to the nullity of the constant c_n, $c_n = 0$) characteristic of the first-order model.

In the general case where n is different from 1 (eq 8), it is finally possible to rearrange the terms to separate $Q(t)$, leading to the general solution

$$\left(1-\frac{Q(t)}{Q_{\mathrm{ads,e}}}\right) = (A\cdot t + B)^{1/1-n} \tag{10}$$

where $A = k_n\cdot(n-1)$ and $B = c_n\cdot(n-1)$. Since at time zero $Q(0) = 0$, this leads in this case to $B = c_n\cdot(n-1) = 1$. Therefore, the general solution of eq 8 can be rewritten as

$$Q(t) = Q_{\mathrm{ads,e}}\cdot[1-(A\cdot t+1)^{1/1-n}] \tag{11}$$

From eq 11, it then becomes possible to fit directly any experimental kinetic curve $Q(t) = f(t)$ and determining the best parameters of fit, namely, the values of $Q_{\mathrm{ads,e}}$, A, and n. As a reminder, this equation is valid only for $n \neq 1$; thus, the case of a first order has *first* to be checked and invalidated before using eq 11. For facilitating the fitting process, the *initial* value of $Q_{\mathrm{ads,e}}$ can be preset (but not fixed) to the apparent stabilization level visually assessed from the $Q(t) = f(t)$ curve.

The application of eq 11 to our experimental kinetic data on the adsorption of TC on a biomimetic apatite led (see Table 1) to better fitting statistics when compared to both the first- and the second-order kinetic models. The best fit using this general model was found for the value $n = 1.4$ (and with $Q_{\mathrm{ads,e}} \approx 41.5$ mg of TC/g of apatite and $A \approx 0.52$ min^{-1}, leading to the approximate rate constant in our experimental conditions of $k = A/(n-1) \approx 1.31$ min^{-1}). Although at this stage it is difficult to draw mechanistic conclusions, the decimal value of n (comprised between 1 and 2) points to a rather complex adsorption process which can probably be related to the heterogeneous adsorbent surface and/or to the presence of several polar groups on the tetracycline molecule. In any case, it appears that, as suggested by Liu and Liu[33] for other types of adsorption systems, the use of a general kinetic model with *no preset* reaction *order* is advisible when dealing with nanocrystalline apatites as adsorbents.

Taking into account the rather complex adsorption behavior observed here (kinetics not following a simple exponential tendency and more likely fitted with a decimal reaction order), the kinetic data were also tentatively fitted with a double-exponential model (DEM), which may be formulated by the following equation

$$Q(t) = Q_{\mathrm{ads,e}} - a_1\cdot\exp(-k_1\cdot t) - a_2\cdot\exp(-k_2\cdot t) \tag{12}$$

Such a DEM model was previously considered to describe the kinetics of adsorption processes involving either two main populations of surface sites or two main parallel kinetic phases (one slower than the other, potentially involving diffusive steps).[31,47] This was, for example, used for describing the adsorption of nucleic acid bases on montmorillonite, a clay material known to expose two types of sites, namely, on the interlayer region of the clay structure and on the faces of the lamella. The application of the DEM model to the present study of TC adsorption on nanocrystalline apatite was checked, and the obtained statistical outcomes were added in Table 1. As can be seen, an adjusted R^2 coefficient of 0.9983 was reached in this case, which is higher than the value (0.9975) obtained for the global kinetic model of order $n = 1.4$. This DEM model was tentatively tested here to investigate whether a multiexponential

DOI: 10.1021/jp5116756
J. Phys. Chem. B XXXX, XXX, XXX−XXX

variation could explain more satisfactorily the observed kinetic data. Taking into account the surface heterogeneity of apatite nanocrystals, it seems indeed reasonable to test also the possibility of having more than one single contribution to the adsorption kinetics. The good fit of the experimental data to a double-exponential model is an indication that our hypothesis may be right.

Although, at this point, it is difficult to assess the two physical origins of this dual model by a lack of mechanistic information, this correlation suggests a situation where a process in (at least) two parallel stages may apply: whether this duality could be linked to the existence of two main types or location of adsorption sites, or of two main molecular orientations, or to other causes is however still undetermined. Additional work on various adsorbent/apatite systems as well as more detailed analysis of the nonapatitic surface layer present on these apatites will be needed to investigate further this point. The good fit obtained with the DEM model might be also linked, at least in some cases, to the existence of more or less accessible sites, making diffusive aspects (e.g., through the sample porosity) non-negligible.[31] A deep exploration of the powder porosity fell out of the scope of this paper; however, it may be noted that BET analysis points to the mesoporous character of such a nanocrystalline apatite powder, with a total pore volume of around 1−1.5 cm^3/g and an average pore diameter around 45 nm. It thus appeared interesting to check whether or not the TC adsorption process was explainable on the basis of a single diffusion step through the porosity. This was inspected by checking if our kinetic data could be fitted by a square-root-of-time relationship (Higuchi-like behavior[48]). This type of $\sqrt{t}$ dependency is indeed often considered for describing kinetic processes limited by diffusion mechanisms (e.g., through a porous or degrading matrix).[32,33,48] Our results clearly indicate (see Table 1) that a unique $k\cdot\sqrt{t}$ variation cannot explain by itself the distribution of experimental data points (adjusted R^2 of 0.6062), showing that the kinetic evolution is not only controlled by TC diffusion, in contrast to what was found in the kinetic study of sludge-derived TC adsorption that was controlled by intraparticle diffusion.[28] However, this does not definitively rule out the existence of diffusive constrains, as diffusion aspects may still be present and take part in the double-exponential variation observed in practice.

In the same philosophy, the Elovich equation (a rather empirical model) was previously associated with adsorption processes on heterogeneous surfaces (e.g., ref [49]), and it thus appeared sensible to assess also the quality of the fit obtained by confronting this model with our experimental data. This equation refers to the relation

$$\frac{dQ(t)}{dt} = a\cdot\exp(-b\cdot Q(t)) \tag{13}$$

where a and b are constants (in the conditions of the experiment), leading to

$$Q(t) = \frac{1}{b}\ln(t + t_0) + \frac{1}{b}\ln(ab) \tag{14}$$

where t_0 is the pre-Elovich factor ($t_0 = 1/ab$), often negligible. The correlation with this model can be checked by following the logarithmic evolution of $Q(t)$ versus t. The Elovich equation was, for example, recently shown to fit rather adequately kinetic data referring to the adsorption of DNA on biomimetic apatite (in anthropology/archeological settings).[50] The fitting statistics found in relation to the Elovich model in the present study have been added in Table 1. The goodness of fit was found to approach the statistics obtained with the second-order equation, with an adjusted R^2 coefficient of 0.9972. Although this model proves to be less accurate than the DEM equation or even the general model with $n = 1.4$ to fit our experimental data, the relatively good fit obtained seems to highlight again the role of the heterogeneous adsorbing apatite surface, especially in the case of a molecule such as tetracycline which does not expose charged end groups with a known high affinity for apatitic surfaces (contrary to phosphate, phosphonate, or carboxylate end groups). TC is however not totally uncharged in our working conditions. It is indeed an amphoteric molecule with ionizable groups (i.e., a tricarbonylamide group, a phenolic diketone group, and a dimethyl amino group, see Figure 1) which can undergo protonation or deprotonation reactions depending on the pH.[26,28] In particular, the formation of a zwitterion has been pointed out[26] for pH values between 3.3 and 7.7 where both the physiological pH and our experimental value are included: in this pH range, tetracycline exists as H_2TC^0 or HTC^- species, suggesting that the positive charge of the dimethylammonium functional group on the TC molecule (due to the protonation of the $-N(CH_3)_2$ group at a pH lower than 9.7, see Figure 1) may contribute to some extent to promote electrostatic interactions between TC and the apatite surface. However, ammonium groups are generally considered to interact only with a low affinity to the surface of apatite.

The above discussion suggests that nanocrystalline apatite surface heterogeneity probably plays an important role on the kinetic evolution experimentally observed here. Considering the Elovich model also allows one to discuss the rate of adsorption. Indeed, Wu et al.[49] investigated in depth 64 adsorption systems (including inorganic and organic adsorbents and ionic and molecular adsorbates) and their Elovich parameters, and these authors classified these systems into four categories (from I to IV) depending on the speed (rate) at which the adsorption took place once establishing the contact between the adsorbate and the adsorbent. A dimensionless version of the Elovich relationship was rewritten for this purpose[49] by adding to the regular equation some reference Q and t values (at high value of t, e.g., close to equilibrium, $Q_{ads,e}$ and t_e). This led to an equation of the form

$$\frac{Q(t)}{Q_{ads,e}} = R_E\cdot\ln\left(\frac{t}{t_e}\right) + 1$$

where R_E (so-called "approaching equilibrium Elovich parameter") decreases when the adsorption rate increases. Calculation of the R_E parameter in our case seems reasonable due to the relatively high correlation coefficient (albeit not the highest) found when fitting our data with this model. It led in our case to $R_E \approx 0.13$. This value is found in category II of Wu et al.'s classification,[49] corresponding to so-called "mild rising" adsorption systems (as for any R_E comprised between 0.1 and 0.3). TC adsorption on nanocrystalline apatite therefore seems to be characterized by a rather intermediate rate of interaction, which might to some extent be linked to the absence of high-affinity charged end groups in the TC molecule formula.

All in all, experimental kinetic data on tetracycline adsorption on nanocrystalline apatite may be best described (in order of goodness of fit) by (1) a double-exponential model (DEM) or by (2) a global kinetic model with a reaction order of $n = 1.4$.

DOI: 10.1021/jp5116756
J. Phys. Chem. B XXXX, XXX, XXX−XXX

This kinetic investigation suggests in all cases that the adsorption of tetracycline molecules (polar but not exposing charged end groups with known high affinity for apatites) on biomimetic apatite is a rather complex phenomenon, probably caused to an important degree by the heterogeneity of the surface of such biomimetic apatites.

3.2.2. TC Adsorption Isotherm. On the basis of the above TC adsorption kinetics overview, contact time was fixed to 100 min in the subsequent adsorption study aiming at determining the whole adsorption isotherm (at ambient temperature, $T \approx 22$ °C).

The adsorption isotherm plotted in Figure 5 as $Q_{ads,e}$ vs the equilibrium concentration C_{eq} is nonlinear. The plot is

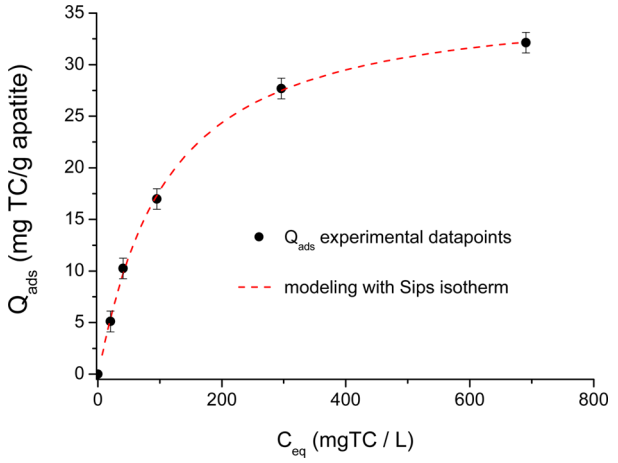

Figure 5. Adsorption isotherm (at 22 °C) of TC on biomimetic apatite matured 1 day and fit with the Sips isotherm model.

characterized by a rather steep increase of the adsorbed amount (up to about 10−15 mg TC/g apatite), followed by a progressive evolution toward stabilization. This general shape corresponds to a situation where adsorbed molecules tend toward monolayer coverage: no indication of a multilayer coverage was detectable.

These experimental data points have then been tentatively fitted to adsorption models encountered/discussed in the literature (e.g., refs 33, 51, and 52) and used for modeling adsorption data. In a first stage, three common models, namely, Langmuir, Freundlich, and Temkin, were considered, these three models being, respectively, described by the following equations

$$Q_{ads,e} = Q_m \cdot \frac{K_L \cdot C_{eq}}{1 + K_L \cdot C_{eq}} \quad \text{Langmuir model} \tag{15}$$

$$Q_{ads,e} = K_F \cdot C_{eq}^{\,1/n} \quad \text{Freundlich model} \tag{16}$$

$$Q_{ads,e} = a \cdot \ln(C_{eq}) + b \quad \text{Temkin model} \tag{17}$$

where K_L, Q_m, K_F, n, a, and b are the corresponding constants at fixed temperature. In order to ease this fitting procedure, the data have been replotted in terms of $1/Q_{ads,e} = f(1/C_{eq})$, $\ln(Q_{ads,e}) = f(\ln(C_{eq}))$, and $Q_{ads,e} = f(\ln(C_{eq}))$, respectively, for the Langmuir, Freundlich, and Temkin models, and the goodness of fit can then be appreciated from the correlation coefficient of the obtained linear relationships. Among these three models, the best correlation was found when the experimental data points were fitted following the Temkin model (correlation coefficient R^2 of 0.9944, with $a = 7.955 \pm 0.345$ and $b = -18.993 \pm 1.680$), while Langmuir and Freundlich led to $R^2 = 0.9930$ and 0.9361, respectively. The Temkin model states that all adsorption sites are not equal in terms of energy; therefore, this good correlation suggests that the adsorption behavior of TC molecules on biomimetic apatite does *not* correspond to one single type of interaction with a constant heat of adsorption independent of the surface sites and/or of the extent of coverage. Instead, the plurality of surface interactions is underlined here. The Temkin isotherm model has been initially built by considering a distribution of surface sites corresponding to decreasing adsorption enthalpies as a function of the coverage (e.g., ref 53) and was used in the literature to describe adsorption data on the adsorption of ionic adsorbents on heterogeneous surfaces (e.g., refs 40−43). However, in the present case where the adsorbate molecules do not expose high-affinity charged end groups (in contrast to most adsorption studies dealing with apatites to this date), the plurality of molecular interactions at the apatite surface could also be in linking with different orientations of the tetracycline and/or with an adsorption behavior which is closely dependent on the coverage (lateral interactions between adsorbed molecules).

Despite a rather high correlation coefficient (0.9944) obtained when fitting the experimental data with a Temkin isotherm, the search for an even better correlation was pursued by testing other models also. The above result was indicative of a situation where the Langmuir hypotheses (single type of adsorption sites corresponding to a constant heat of adsorption, up to monolayer coverage, absence of lateral interaction) did not strictly apply. It was consequently interesting at this point to check whether a modification of the Langmuir isotherm could allow a better fit. In this view, the so-called Sips isotherm, also named the Langmuir−Freundlich isotherm, has been proposed and used to model adsorption processes (e.g., refs 33 and 54)

$$Q_{ads,e} = Q_m \cdot \frac{K_S \cdot C_{eq}^{\,m}}{1 + K_S \cdot C_{eq}^{\,m}} \quad \text{ips isotherm} \tag{18}$$

where the Sips parameter m is the main alteration of eq 15 (the value $m = 1$ corresponding to a Langmuir isotherm). Note that in some reports, the Sips constant appearing in the equation is expressed with the exponent m as $(K_S')^m$. At high coverage, $K_s \cdot C_{eq}^{\,m}$ becomes significantly greater than 1; therefore, the system tends toward a monolayer coverage as in regular Langmuir; whereas at low coverage, $K_s \cdot C_{eq}^{\,m} \ll 1$ and eq 18 then resembles the Freundlich isotherm (eq 16). Equation 18 can be rewritten as

$$\ln\left[\frac{Q_{ads,e}}{Q_m - Q_{ads,e}}\right] = \ln(K_S) + m \cdot \ln(C_{eq}) \tag{19}$$

which allows one to test the correlation with this model by checking the linearity of the plot $\ln[Q_{ads,e}/(Q_m - Q_{ads,e})] = f(\ln(C_{eq}))$ after estimating visually the asymptote value, Q_m. A more formal fitting program can however be alternatively used (and should be preferred), thanks to the following rewriting (by extracting $Q_{ads,e}$ from eq 19 and expressing it versus C_{eq})

$$Q_{ads,e} = Q_m \cdot \frac{\exp \psi}{1 + \exp \psi} \tag{20}$$

and noting

DOI: 10.1021/jp5116756
J. Phys. Chem. B XXXX, XXX, XXX−XXX

$$\psi = \exp(\ln(K_S) + m\cdot\ln(C_{eq})) \quad (21)$$

Applying eqs 20 and 21 to our experimental data leads to a regression coefficient very close to unity (R^2 = 0.9990). This indicates an excellent match to the Sips isotherm (significantly improved over the Temkin model). The fitted Sips parameters were found as follows: m = 1.08 ± 0.06, Q_m = 36.4 ± 1.1 mg/g, and K_S = 0.0067 ± 0.0014 (for C expressed in mg/L) which is equivalent to K_S = 8515.6 ± 1.2 (for C expressed in mol/L).

The value of Q_m is thus found to reach ∼36.4 mg per gram of nanocrystalline, noncarbonated apatite matured 1 day at room temperature. In moles, this value corresponds to 0.082 mmol/g (molecular weight of TC 444.4 g/mol) or, per m^2, 0.68 μmol/m^2 (apatite specific surface area close to 120 m^2/g). At this point, it may appear tempting to try to compare this value to other adsorption cases. This is however not trivial when the adsorbent is a nanocrystalline apatite, as such apatites can exhibit very different physicochemical features and surface reactivities depending on their maturation state (which itself depends on synthesis conditions,[3] as discussed in the Introduction). Data from the literature obtained for the adsorption of other molecules/drugs on "nanosized" apatite substrates may however be recalled, at least for a comparison of maximum adsorbed amounts. An adsorption plateau was, for example, found around 0.7 μmol/m^2 when considering the adsorption of terbium complexes of organic ligands,[55] which is of the same order as the one found here to tetracycline. In contrast, greater Q_m values were, for example, reported, leading (after recalculation in μmol/m^2) to 2.7 μmol/m^2 for tiludronate[56,57] (a bisphosphonate compound exhibiting phosphonate groups with a high affinity for the surface of apatite), to ∼2.4 μmol/m^2 for platinum bisphosphonate complexes,[12] to ∼2.2 μmol/m^2 for trimethylenephosphonate−polyethylenimine,[58] or even to ∼8.2 μmol/m^2 for doxorubicin.[59] The observation of rather low adsorbed amounts for tetracycline is however rather not surprising, taking into account the lack of known high-affinity groups on the formula of tetracycline.

The value of m (1.08) found here differs somewhat from unity, thus supporting the need to "inject some Freundlich behavior" in regular Langmuir to correctly fit our data, which was similarly done previously for other liquid/solid systems (e.g., refs 33 and 54). These literature works discussed, from an applied viewpoint, the physical meaning of the parameters m and K_S from the Sips adsorption model. The fact that m is different from unity may be related to the heterogeneous character of the surface. The value of m may however also give some insight on the level of "cooperativity" between adjacent adsorbed species, involving lateral interactions[54] (with m > 1 for "positive" cooperativity and m < 1 for "negative" cooperativity, as determined for theoretically homogeneous initial surfaces). In our case, the value of m, greater than unity, could in fact denote both some degree of surface heterogeneity in the accessible adsorption sites *and* a non-negligible role of lateral interactions (positive role of adsorbed molecules on the adsorption of further molecules). Positive cooperativity was also found for the adsorption of proteins on hydroxyapatite by Luo and Andrade[60] (in that work, the Sips isotherm was used by the authors in another form known as the Hill equation). The existence of many polar groups in various parts of the TC molecule probably favors the formation of lateral cooperativity in the adsorption process; however, without the input of computational chemistry, for example, it appears delicate at this point to propose here specific molecular orientations of the TC molecule at the surface of apatite nanocrystals.

The value of K_S has also been shown to bear some thermodynamic meaning, being related to the change in standard Gibbs free energy of adsorption; the overall change in free energy being the driving force of the adsorption process. Liu et al.[33] pointed out that the following relation applied (for a value of K_S determined from C in mol/L)

$$K_S = \exp\left(-\frac{\Delta G_{ads}^{\circ}}{RT}\right) \quad (22)$$

In our case, this equation leads to $\Delta G_{ads}^{\circ} \cong -22$ kJ/mol (uncertainty estimated to ±1 kJ/mol). This negative value points to a situation where the adsorption process (TC on biomimetic apatite) is favored *in standard conditions*. According to Liu et al.,[33] the *overall effective change* of free energy, ΔG_{abs}, can then be calculated for any condition during the adsorption process (corresponding to concentration in solution of C, mol/L, and to an adsorbed amount Q_{ads}) from the relation

$$\Delta G_{ads} = \Delta G_{ads}^{\circ} - mRT\cdot\ln(C) + RT\cdot\ln\left[\frac{Q_{ads}}{Q_{th} - Q_{ads}}\right] \quad (23)$$

where Q_{th} is the maximum theoretical capacity (expressed in the same unit as Q_{ads}, here in mg/g), R is the gas constant (8.314 J·mol^{-1}·K^{-1}), T is the absolute temperature in Kelvin, and m is the exponent of the Sips isotherm. Considering that $Q_{th} = Q_m$ (= saturation level of the isotherm), eq 23 allows one to verify that, at equilibrium (i.e., for $C = C_{eq}$ and $Q_{ads} = Q_{ads,e}$), the values of ΔG_{ads} are close to zero. This was indeed the case in the present work, where values of ΔG_{ads} at equilibrium, calculated using eq 23, were systematically found close to zero, between 0 and 0.7 kJ/mol (±1 kJ/mol) for all data points. Negative values of ΔG_{ads} then occur during the whole TC adsorption process (up to reaching 0 at equilibrium). For instance, when 1000th (1/1000th) of the total adsorption amount is reached (calculated, for example, for any initial concentration down to 10^{-10} mol/L), which is around the initiation of the adsorption process, ΔG_{ads} ranges between −34 and −30 kJ/mol. It may be noted that such ΔG_{ads} values fall close to the limit between physisorption and chemisorption.[61] Taking into account the absence of an "obvious" high-affinity charged end group on the TC molecules, it appears reasonable to consider that these non-negligible negative values probably originate not only from substrate/molecule interactions at the adsorption sites but also from stabilizing (positive) lateral contributions, as suggested above by the m > 1 value of the Sips parameter.

3.2.3. TC Release Experiment in Aqueous Medium (Neutral pH). The above results indicate the possibility to adsorb TC molecules, in a controlled and describable way, on the surface of a nanocrystalline biomimetic apatite. This may present an applied interest, for example, in the field of bone regeneration and infection control. It was thus interesting, at this point, to inspect (in a preliminary way here) the TC release behavior in aqueous medium. In order to privilege a situation where solely the adsorption/desorption of TC would come into play (absence of competitive molecular adsorption), this release experiment was undergone in deionized water, set to neutral pH, in the absence of any foreign molecules.

The experimental setup is detailed in the Materials and Methods. Briefly, a pellet of TC-loaded apatite was first

DOI: 10.1021/jp5116756
J. Phys. Chem. B XXXX, XXX, XXX−XXX

prepared (mass of pellet 96 mg, initial concentration in TC during adsorption 490 mg/L, corresponding to an equilibrium concentration during the adsorption experiment of 362 mg/L and to an adsorbed amount Q_{ads} of 32.4 mg TC/g apatite). Consequently, the TC-loaded pellet of 96 mg contained a total of 3.11 mg of TC, distributed throughout the pelletized powder. The pellet was introduced in a recirculation cell (total volume of medium 50 mL), and the TC concentration transferred to the medium versus time was measured. Figure 6 reports the plot of the measured TC concentration versus

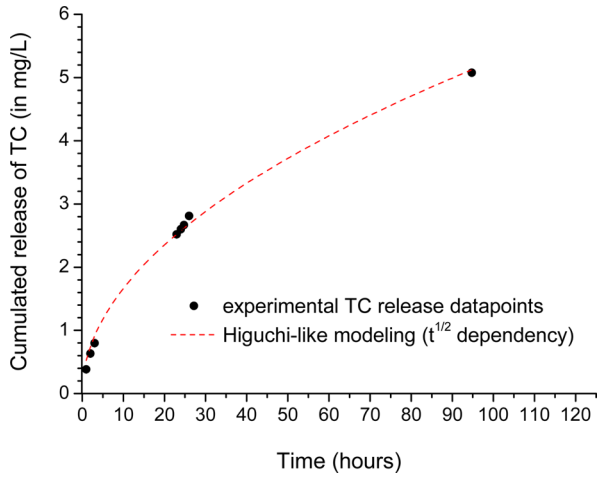

Figure 6. TC release from pelletized nanocrystalline apatite in recirculation cell (water, ambient temperature, neutral pH).

time. The release is found to be initiated immediately after immersion in aqueous medium and is continuous with time with a progressive decrease of release rate as usually in release studies.

The data points have been tentatively fitted to mathematical models often encountered in release profile fitting and described, for example, by Costa.[62] The plot could not be reasonably fitted to neither zero-order (R^2 = 0.886) nor first-order (R^2 = 0.611) models, as the cumulated released TC concentration ($C_{cumulated}$) or its logarithm did not vary linearly with time. Also, only a poor linear correlation (R^2 = 0.930) was found between $\ln(-dQ_{ads}/dt)$ and ($\ln Q_{ads}$), where $Q_{ads}(t)$ is the remaining adsorbed amount at time t, thus indicating that a "simple" desorption model describable by the following equation (as in the case of the desorption of a gaseous molecule, for example) did not apply here

$$r_d = -\frac{dQ_{ads}(t)}{dt} = \alpha \cdot [Q_{ads}(t)]^p \cdot \exp\left(-\frac{E_d}{RT}\right) \quad (24)$$

where r_d is the rate of desorption, α is the pre-exponential factor, p is the order of the desorption kinetics, and E_d is the activation energy of the desorption process. The plot was then tentatively fitted to the rather general Korsmeyer–Peppas model,[62] with a power dependency of the type $C_{cumulated} = a \cdot t^b$. A high level of correlation was then found (R^2 = 0.997), with the fitted values a = 0.510 ± 0.033 and b = 0.509 ± 0.017. It may be remarked that the value of b is very close to 0.5, therefore suggesting that the kinetics of release could in fact be described, at least in a first good approximation, by a Fick diffusion model in $\sqrt{t}$, corresponding to the Higuchi model[48] which is a particular case of Korsmeyer–Peppas modeling. This observation thus suggests that a diffusion phenomenon could be the rate-limiting step in the present release study. Taking into account both the rather small size of tetracycline molecules and the pelletizing of the powder, diffusion through intercrystalline porosity appears indeed expectable in this case.

3.3. CONCLUSIONS

This study investigated in depth the adsorption process of tetracycline molecules (polar but not exhibiting known high-affinity end groups for apatite surfaces) on a biomimetic nanocrystalline apatite. We showed that this antibiotic molecule/substrate association followed a well-determined adsorption process, despite rather low adsorbed amounts as compared to molecules exposing end groups like phosphonates, for example. The kinetics of adsorption could be best fitted to a double-exponential model or otherwise to a general kinetic equation with a decimal reaction order (n = 1.4), pointing out in all cases a rather complex adsorption phenomenon. The adsorption isotherm could be perfectly described on the basis of the Sips model (aka Langmuir–Freundlich) with an exponent coefficient greater than unity ($m \cong 1.08$), highlighting the heterogeneity of the surface and suggesting also some degree of cooperativity between adjacent adsorbed molecules. The (negative) change in Gibbs free energy of adsorption was also evaluated from the Sips parameters; it indicates a situation close to the limit between simple physisorption (not multilayer in this case) and chemisorption.

The use of tetracycline-loaded scaffolds based on nanocrystalline biomimetic apatites may therefore be envisioned in the future. In a preliminary experiment, the release of TC molecules was studied in water at neutral pH (in the absence of competing species) so as to examine the release profile. In our experimental conditions, using pelletized TC-loaded nanocrystalline apatite, TC molecules were found to be released progressively and following a Higuchi-like behavior pointing out a rate-limiting step of diffusive nature. This study should prove helpful for a better understanding of the interaction of polar molecules and biomimetic apatites and, in particular, for the setup of bone scaffolds functionalized by way of molecular adsorption, e.g., in view of the release of adsorbed drugs directly on the implantation site.

AUTHOR INFORMATION

Corresponding Author

*Phone: +33 (0)5 34 32 34 11. E-mail: christophe.drouet@ensiacet.fr.

Notes

The authors declare no competing financial interest.

ACKNOWLEDGMENTS

The authors thank Ms. Camille Fastre for experimental support and the *BioCapabili engineering cluster on Innovative Antimicrobial Materials* (www.biocapabili.com) for scientific discussions.

REFERENCES

(1) Elliott, J. C. *Structure and Chemistry of the Apatites and Other Calcium Orthophosphates*; Elsevier Science: Amsterdam, 1994; Vol. *18*.
(2) LeGeros, R. Z. Calcium Phosphate-Based Osteoinductive Materials. *Chem. Rev.* **2008**, *108*, 4742–4753.
(3) Vandecandelaere, N.; Rey, C.; Drouet, C. Biomimetic Apatite-based Biomaterials: On the Critical Impact of Synthesis and Post-synthesis Parameters. *J. Mater. Sci.-Mater. Med.* **2012**, *23*, 2593–2606.

DOI: 10.1021/jp5116756
J. Phys. Chem. B XXXX, XXX, XXX–XXX

(4) Cazalbou, S.; Combes, C.; Eichert, D.; Rey, C.; Glimcher, M. J. Poorly Crystalline Apatites: Evolution and Maturation In Vitro and In Vivo. *J. Bone Miner. Metab.* **2004**, *22*, 310−317.
(5) Eichert, D.; Combes, C.; Drouet, C.; Rey, C. Formation and Evolution of Hydrated Surface Layers of Apatites. *Bioceramics* **2005**, *17*, 3−6.
(6) Weber, C. G.; Mueller, M.; Vandecandelaere, N.; Trick, I.; Burger-Kentischer, A.; Maucher, T.; Drouet, C. Enzyme-functionalized Biomimetic Apatites: Concept and Perspectives in View of Innovative Medical Approaches. *J. Mater. Sci.-Mater. Med.* **2014**, *25*, 595−606.
(7) Errassifi, F.; Sarda, S.; Barroug, A.; Legrouri, A.; Sfihi, H.; Rey, C. Infrared, Raman and NMR Investigations of Risedronate Adsorption on Nanocrystalline Apatites. *J. Colloid Interface Sci.* **2014**, *420*, 101−111.
(8) Bosco, R.; Iafisco, M.; van den Beucken, J.; Leeuwenburgh, S.; Jansen, J. Adsorption of Alendronate onto Biomimetic Apatite Nanocrystals to Develop Drug Carrier Coating for Bone Implants. *Bioceramics* **2013**, *529−530*, 475−479.
(9) Autefage, H.; Briand-Mesange, F.; Cazalbou, S.; Drouet, C.; Fourmy, D.; Goncalves, S.; Salles, J.; Combes, C.; Swider, P.; Rey, C. Adsorption and Release of BMP-2 on Nanocrystalline Apatite-Coated and Uncoated Hydroxyapatite/beta-Tricalcium Phosphate Porous Ceramics. *J. Biomed. Mater. Res., B* **2009**, *91B*, 706−715.
(10) Xu, H. H. K.; Weir, M. D.; Simon, C. G. Injectable and Strong Nano-apatite Scaffolds for Cell/Growth Factor Delivery and Bone Regeneration. *Dent. Mater.* **2008**, *24*, 1212−1222.
(11) Drouet, C.; Carayon, M.-T.; Combes, C.; Rey, C. Surface Enrichment of Biomimetic Apatites with Biologically-active Ions Mg^{2+} and Sr^{2+}: A Preamble to the Activation of Bone Repair Materials. *Mater. Sci. Eng., C* **2008**, *28*, 1544−1550.
(12) Iafisco, M.; Palazzo, B.; Martra, G.; Margiotta, N.; Piccinonna, S.; Natile, G.; Gandin, V.; Marzano, C.; Roveri, N. Nanocrystalline Carbonate-apatites: Role of Ca/P Ratio on the Upload and Release of Anticancer Platinum Bisphosphonates. *Nanoscale* **2012**, *4*, 206−217.
(13) Iafisco, M.; Margiotta, N. Silica Xerogels and Hydroxyapatite Nanocrystals for the Local Delivery of Platinum-bisphosphonate Complexes in the Treatment of Bone Tumors: A Mini-review. *J. Inorg. Biochem.* **2012**, *117*, 237−247.
(14) Drouet, C.; Gómez-Morales, J.; Iafisco, M.; Sarda, S. Calcium Phosphate Surface Tailoring Technologies for Drug Delivering and Tissue Engineering and applied aspects. In *Surface Tailoring of Inorganic Materials for Biomedical Applications*; Rimondini, L., Bianchi, C. L., Verne, E., Eds.; Bentham Science: Oak Park, IL, 2012.
(15) Gomez-Morales, J.; Iafisco, M.; Manuel Delgado-Lopez, J.; Sarda, S.; Drouet, C. Progress on the Preparation of Nanocrystalline Apatites and Surface Characterization: Overview of Fundamental and Applied Aspects. *Prog. Cryst. Growth Charact. Mater.* **2013**, *59*, 1−46.
(16) Gautier, H.; Plumecocq, A.; Amador, G.; Weiss, P.; Merle, C.; Bouler, J. M. In Vitro Characterization of Calcium Phosphate Biomaterial Loaded with Linezolid for Osseous Bone Defect Implantation. *J. Biomater. Appl.* **2012**, *26*, 811−828.
(17) de Souza, C. A. S.; Colombo, A. P. V.; Souto, R. M.; Silva-Boghossian, C. M.; Granjeiro, J. M.; Alves, G. G.; Rossi, A. M.; Rocha-Leao, M. H. M. Adsorption of Chlorhexidine on Synthetic Hydroxyapatite and In Vitro Biological Activity. *Colloids Surf., B* **2011**, *87*, 310−318.
(18) Hesaraki, S.; Zamanian, A.; Khorami, M. Nano-Structured Apatite Granules as Drug Delivery Device for Bone Infection Treatments. *J. Aust. Ceram. Soc.* **2011**, *47*, 32−36.
(19) Schneider, O. D.; Loher, S.; Brunner, T. J.; Schmidlin, P.; Stark, W. J. Flexible, Silver Containing Nanocomposites for the Repair of Bone Defects: Antimicrobial Effect Against E. Coli Infection and Comparison to Tetracycline Containing Scaffolds. *J. Mater. Chem.* **2008**, *18*, 2679−2684.
(20) Meng, D.; Francis, L.; Thompson, I. D.; Mierke, C.; Huebner, H.; Amtmann, A.; Roy, I.; Boccaccini, A. R. Tetracycline-encapsulated P(3HB) Microsphere-coated 45S5 Bioglass(A (R))-based Scaffolds for Bone Tissue Engineering. *J. Mater. Sci.-Mater. Med.* **2013**, *24*, 2809−2817.
(21) Gee, A.; Dietz, V. R. Determination of Phosphate by Differential Spectrophotometry. *Ann. Chem.* **1953**, *25*, 1320−1324.
(22) Drouet, C. Apatite Formation: Why It May Not Work as Planned, and How to Conclusively Identify Apatite Compounds. *Biomed Res. Int.* **2013**, *12*, Article ID 490946, pp 1−12.
(23) Rey, C.; Marsan, O.; Combes, C.; Drouet, C.; Grossin, D.; Sarda, S. Characterization of Calcium Phosphates Using Vibrational Spectroscopies. In *Advances in Calcium Phosphate Biomaterials*, Ben-Nissan, B., Ed.; Springer: Berlin Heidelberg, 2014; Vol. 2, pp 229−266.
(24) Rey, C.; Lian, J.; Grynpas, M.; Shapiro, F.; Zylberberg, L.; Glimcher, M. J. Non-apatitic Environments in Bone Mineral: FT-IR Detection, Biological Properties and Changes in Several Disease States. *Connect. Tissue Res.* **1989**, *21*, 267−273.
(25) Rey, C.; Hina, A.; Tofighi, A.; Glimcher, M. J. Maturation of Poorly Crystalline Apatites: Chemical and Structural Aspects In Vivo and In Vitro. *Cells Mater.* **1995**, *5*, 345−356.
(26) Chang, P.-H.; Li, Z.; Jiang, W.-T.; Kuo, C.-Y.; Jean, J.-S. Adsorption of Tetracycline on Montmorillonite: Influence of Solution pH, Temperature, and Ionic Strength. *Desalin. Water Treat.* **2014**, 1−13 DOI: 10.1080/19443994.2014.924881.
(27) Chang, P. H.; Li, Z. H.; Jean, J. S.; Jiang, W. T.; Wang, C. J.; Lin, K. H. Adsorption of Tetracycline on 2:1 Layered Non-Swelling Clay Mineral Illite. *Appl. Clay Sci.* **2012**, *67−68*, 158−163.
(28) Ocampo-Perez, R.; Rivera-Utrilla, J.; Gomez-Pacheco, C.; Sanchez-Polo, M.; Lopez-Penalver, J. J. Kinetic Study of Tetracycline Adsorption on Sludge-Derived Adsorbents in Aqueous Phase. *Chem. Eng. J.* **2012**, *213*, 88−96.
(29) Zhao, Y.; Geng, J.; Wang, X.; Gu, X.; Gao, S. Adsorption of Tetracycline onto Goethite in the Presence of Metal Cations and Humic Substances. *J. Colloid Interface Sci.* **2011**, *361*, 247−251.
(30) Zhang, L.; Song, X.; Liu, X.; Yang, L.; Pan, F.; Lv, J. Studies on the Removal of Tetracycline by Multi-walled Carbon Nanotubes. *Chem. Eng. J.* **2011**, *178*, 26−33.
(31) Qiu, H.; Lv, L.; Pan, B. C.; Zhang, Q. J.; Zhang, W. M.; Zhang, Q. X. Critical Review in Adsorption Kinetic Models. *J. Zhejiang Univ.-Sci. A* **2009**, *10*, 716−724.
(32) Sen Gupta, S.; Bhattacharyya, K. G. Kinetics of Adsorption of Metal Ions on Inorganic Materials: A Review. *Adv. Colloid Interface Sci.* **2011**, *162*, 39−58.
(33) Liu, Y. Biosorption Isotherms, Kinetics and Thermodynamics. *Sep. Purif. Technol.* **2008**, *61*, 229−242.
(34) Genc-Fuhrman, H.; Tjell, J. C.; McConchie, D. Adsorption of Arsenic from Water using Activated Neutralized Red Mud. *Environ. Sci. Technol.* **2004**, *38*, 2428−2434.
(35) Gupta, V. K.; Sharma, S. Removal of Cadmium and Zinc from Aqueous Solutions using Red Mud. *Environ. Sci. Technol.* **2002**, *36*, 3612−3617.
(36) Gupta, V. K.; Gupta, M.; Sharma, S. Process Development for the Removal of Lead and Chromium from Aqueous Solutions using Red Mud - An Aluminium Industry Waste. *Water Res.* **2001**, *35*, 1125−1134.
(37) Gimenez, J.; Martinez, M.; de Pablo, J.; Rovira, M.; Duro, L. Arsenic Sorption onto Natural Hematite, Magnetite, and Goethite. *J. Hazard. Mater.* **2007**, *141*, 575−580.
(38) Mathialagan, T.; Viraraghavan, T. Adsorption of Cadmium from Aqueous Solutions by Perlite. *J. Hazard. Mater.* **2002**, *94*, 291−303.
(39) Sari, A.; Tuzen, M. Removal of Cr(VI) From Aqueous Solution by Turkish Vermiculite: Equilibrium, Thermodynamic and Kinetic Studies. *Sep. Sci. Technol.* **2008**, *43*, 3563−3581.
(40) Ghadim, E. E.; Manouchehri, F.; Soleimani, G.; Hosseini, H.; Kimiagar, S.; Nafisi, S. Adsorption Properties of Tetracycline onto Graphene Oxide: Equilibrium, Kinetic and Thermodynamic Studies. *PLoS One* **2013**, *8*, 1−9.
(41) Dai, J. D.; Wei, X.; Cao, Z. J.; Zhou, Z. P.; Yu, P.; Pan, J. M.; Zou, T. B.; Li, C. X.; Yan, Y. S. Highly-controllable Imprinted Polymer Nanoshell at the Surface of Magnetic Halloysite Nanotubes for Selective Recognition and Rapid Adsorption of Tetracycline. *RSC Adv.* **2014**, *4*, 7967−7978.

DOI: 10.1021/jp5116756
J. Phys. Chem. B XXXX, XXX, XXX−XXX

(42) Xu, Z. Y.; Fan, J.; Zheng, S. R.; Ma, F. F.; Yin, D. Q. On the Adsorption of Tetracycline by Calcined Magnesium-Aluminum Hydrotalcites. *J. Environ. Qual.* **2009**, *38*, 1302−1310.
(43) Bahdod, A.; El Asri, S.; Saoiabi, A.; Coradin, T.; Laghzizil, A. Adsorption of Phenol from an Aqueous Solution by Selected Apatite Adsorbents: Kinetic Process and Impact of the Surface Properties. *Water Res.* **2009**, *43*, 313−318.
(44) Bogya, E. S.; Cziko, M.; Szabo, G.; Barabas, R. The Red Beetroot Extract Antioxidant Activity and Adsorption Kinetics onto Hydroxyapatite-based Materials. *J. Iran. Chem. Soc.* **2013**, *10*, 491−503.
(45) Gomwe, T.; Booth, S. E.; Nicholson, J. W. The Kinetics of Fluoride Uptake by Synthetic Hydroxyapatite. *Ceramics-Silikaty* **2012**, *56*, 85−88.
(46) Ricci, L. Adjusted-squared Type Measure for Exponential Dispersion Models. *Stat. Probab. Lett.* **2010**, *80*, 1365−1368.
(47) Sciascia, L.; Liveri, M. L. T.; Merli, M. Kinetic and Equilibrium Studies for the Adsorption of Acid Nucleic Bases onto K10 Montmorillonite. *Appl. Clay Sci.* **2011**, *53*, 657−668.
(48) Siepmann, J.; Peppas, N. A. Higuchi equation: Derivation, Applications, Use and Misuse. *Int. J. Pharm.* **2011**, *418*, 6−12.
(49) Wu, F. C.; Tseng, R. L.; Juang, R. S. Characteristics of Elovich Equation Used for the Analysis of Adsorption Kinetics in Dye-chitosan Systems. *Chem. Eng. J.* **2009**, *150*, 366−373.
(50) Grunenwald, A.; Keyser, C.; Sautereau, A. M.; Crubezy, E.; Ludes, B.; Drouet, C. Adsorption of DNA on Biomimetic Apatites: Toward the Understanding of the Role of Bone and Tooth Mineral on the Preservation of Ancient DNA. *Appl. Surf. Sci.* **2014**, *292*, 867−875.
(51) Ringot, D.; Lerzy, B.; Chaplain, K.; Bonhoure, J. P.; Auclair, E.; Larondelle, Y. In Vitro Biosorption of Ochratoxin A on the Yeast Industry by-products: Comparison of Isotherm Models. *Bioresour. Technol.* **2007**, *98*, 1812−1821.
(52) Vijayaraghavan, K.; Padmesh, T. V. N.; Palanivelu, K.; Velan, M. Biosorption of Nickel(II) ions onto Sargassum Wightii: Application of Two-parameter and Three-parameter Isotherm Models. *J. Hazard. Mater.* **2006**, *133*, 304−308.
(53) Bolis, V.; Morterra, C.; Fubini, B.; Ugliengo, P.; Garrone, E. Temkin-type Model for the Description of Induced Heterogeneity: CO Adsorption on Group 4 Transition Metal Dioxides. *Langmuir* **1993**, *9*, 1521−1528.
(54) Koopal, L. K.; Vanriemsdijk, W. H.; Dewit, J. C. M.; Benedetti, M. F. Analytical Isotherm Equations for Multicomponent Adsorption to Heterogeneous Surfaces. *J. Colloid Interface Sci.* **1994**, *166*, 51−60.
(55) Rill, C.; Kolar, Z. I.; Kickelbick, G.; Wolterbeek, H. T.; Peters, J. A. Kinetics and Thermodynamics of Adsorption on Hydroxyapatite of the Tb-160 Terbium Complexes of the Bone-Targeting Ligands DOTP and BPPED. *Langmuir* **2009**, *25*, 2294−2301.
(56) Pascaud, P.; Gras, P.; Coppel, Y.; Rey, C.; Sarda, S. Interaction Between a Bisphosphonate, Tiludronate, and Biomimetic Nanocrystalline Apatites. *Langmuir* **2013**, *29*, 2224−2232.
(57) Al-Kattan, A.; Errassifi, F.; Sautereau, A.; Sarda, S.; Dufour, P.; Barroug, A.; Dos Santos, I.; Combes, C.; Grossin, D.; Rey, C.; Drouet, C. Medical Potentialities of Biomimetic Apatites through Adsorption, Ionic Substitution, and Mineral/Organic Associations: Three Illustrative Examples. *Adv. Eng. Mater.* **2010**, *12*, B224−B233.
(58) Jansen, D. R.; Zeevaart, J. R.; Denkova, A.; Kolar, Z. I.; Krijger, G. C. Hydroxyapatite Chemisorption of N,N′,N′-Trimethylene-phosphonate-Poly(ethyleneimine) (PEI-MP) Combined with Sn^{2+} or Sn^{4+}. *Langmuir* **2009**, *25*, 2790−2796.
(59) Rodriguez-Ruiz, I.; Manuel Delgado-Lopez, J.; Duran-Olivencia, M. A.; Iafisco, M.; Tampieri, A.; Colangelo, D.; Prat, M.; Gomez-Morales, J. pH-Responsive Delivery of Doxorubicin from Citrate-Apatite Nanocrystals with Tailored Carbonate Content. *Langmuir* **2013**, *29*, 8213−8221.
(60) Luo, Q. L.; Andrade, J. D. Cooperative Adsorption of Proteins onto Hydroxyapatite. *J. Colloid Interface Sci.* **1998**, *200*, 104−113.
(61) Al-Anber, M. A. In *Thermodynamics-Interaction Studies-Solids, Liquids and Gases*; Moreno-Pirajan, J. C., Ed.; InTech: Rijeka, Croatia, 2011; pp 737−764.
(62) Costa, P.; Sousa Lobo, J. M. Modeling and Comparison of Dissolution Profiles. *Eur. J. Pharm. Sci.* **2001**, *13*, 123−133.

DOI: 10.1021/jp5116756
J. Phys. Chem. B XXXX, XXX, XXX−XXX